

Nitrate addition to groundwater impacted by ethanol-blended fuel accelerates ethanol removal and mitigates the associated metabolic flux dilution and inhibition of BTEX biodegradation

Henry Xavier Corseuil^{a*}, Diego E. Gomez^b, Cássio Moraes Schambeck^a, Débora Toledo Ramos^a
and Pedro J.J. Alvarez^c

^a Federal University of Santa Catarina, Department of Sanitary and Environmental Engineering, Florianópolis, Santa Catarina, Brazil.

^b University of Exeter, Centre for Water Systems, Exeter, Devon, EX4 4QF, United Kingdom.

^c Department of Civil and Environmental Engineering, Rice University, MS-317, 6100 Main St., Houston, TX 77005, USA

*CORRESPONDING AUTHOR. University of Santa Catarina, Department of Sanitary and Environmental Engineering, Florianópolis, Santa Catarina, Brazil, CEP: 88040-970, e-mail: henry.corseuil@ufsc.br
Phone: + 5548-3721-2130, Fax: + 5548 3234-6459 (H.X.C.)

HIGHLIGHTS:

- The attenuation of two controlled ethanol-blended fuel releases were monitored
- One release was biostimulated with nitrate as terminal electron acceptor
- This accelerated removal of ethanol and its inhibitory effect on BTEX degradation
- Preferential ethanol degradation was explained by the metabolic flux dilution model
- Thus, bioremediation efforts targeting ethanol first would also remove BTEX earlier

1 **ABSTRACT**

2 A comparison of two controlled ethanol-blended fuel releases under monitored natural
3 attenuation (MNA) versus nitrate biostimulation (NB) illustrates the potential benefits of
4 augmenting the electron acceptor pool with nitrate to accelerate ethanol removal and thus
5 mitigate its inhibitory effects on BTEX biodegradation. Groundwater concentrations of ethanol
6 and BTEX were measured 2 m downgradient of the source zones. In both field experiments,
7 initial source-zone BTEX concentrations represented less than 5% of the dissolved total organic
8 carbon (TOC) associated with the release, and measurable BTEX degradation occurred only after
9 the ethanol fraction in the multicomponent substrate mixture decreased sharply. However,
10 ethanol removal was faster in the nitrate amended plot (1.4 years) than under natural attenuation
11 conditions (3.0 years), which led to faster BTEX degradation. This reflects, in part, that an
12 abundant substrate (ethanol) can dilute the metabolic flux of target pollutants (BTEX) whose
13 biodegradation rate eventually increases with their relative abundance after ethanol is
14 preferentially consumed. The fate and transport of ethanol and benzene was accurately simulated
15 in both releases using RT3D with our general substrate interaction module (GSIM) that considers
16 metabolic flux dilution. Since source zone benzene concentrations are relatively low compared
17 to those of ethanol (or its degradation byproduct, acetate), our simulations imply that the initial
18 focus of cleanup efforts (after free-product recovery) should be to stimulate the degradation of
19 ethanol (e.g., by nitrate addition) to decrease its fraction in the mixture and speed up BTEX
20 biodegradation.

21

22 **Keywords:** Mixed substrates, BTEX, fuel ethanol, metabolic flux, natural attenuation, GSIM.

23 INTRODUCTION

24 Environmental contamination by single compounds rather than mixtures is uncommon, and
25 microorganisms often face complex mixtures of potential organic substrates. For example, fuel
26 releases contain a wide variety of compounds, including the relatively water-soluble and toxic
27 BTEX compounds (e.g., benzene, toluene, ethylbenzene and xylenes). Unlike the less soluble
28 hydrocarbons in gasoline that exhibit limited migration potential, BTEX concentrations in
29 impacted groundwater are commonly monitored to assess risk and determine the need for
30 remediation.

31 Ethanol is increasingly being used as a fuel additive to alleviate dependence on imported
32 oil and greenhouse gas emissions due to fossil fuel combustion (Goldemberg, 2007), which
33 increases the likelihood of ethanol-blended fuel releases. Preferential degradation of ethanol and
34 its high electron acceptor demand may decrease the rate of BTEX degradation and increase
35 plume reach (Chen et al., 2008; Corseuil et al., 1998; Da Silva & Alvarez, 2004; Gomez et al.,
36 2008; Mackay et al., 2006; Ruiz-Aguilar et al., 2002; Schaefer et al., 2010).

37 Although the molecular structure of a compound can significantly influence its susceptibility to
38 degradation (Alvarez & Illman, 2006), the relative biodegradability of a compound in a mixture of
39 alternative substrates (as reflected by degradation rates) is often a concentration-dependent phenomenon
40 (Egli, 1995). Specifically, the relative abundance of alternative substrates in a mixture can significantly
41 influence biodegradation rates of the compound of interest (Lendenmann et al., 1996; Bielefeldt &
42 Stensel, 1999; Lovanh et al., 2002; Dou et al., 2008; Freitas et al. 2011). For example, higher
43 proportions of toluene in various mixtures of toluene and ethanol result in higher toluene
44 biodegradation rates (Lovanh et al. 2002). This phenomenon, termed metabolic flux dilution
45 (Lovanh & Alvarez, 2004), is a form of noncompetitive inhibition of the degradation of a target
46 substrate due to the metabolism of another (likely initiated by different enzymes). This

47 hindrance by alternative substrates in the mixture (e.g., ethanol) can be accounted by using the
48 metabolic flux dilution factor, which is calculated as the aqueous concentration of a target
49 substrate divided by the total concentration of other dissolved species, expressed as total organic
50 carbon (TOC):

$$51 \quad f = S_{TOC} / T_{TOC} = r_i / r_0 \quad \text{Equation (1)}$$

52 where f is the metabolic flux dilution factor (dimensionless), S_{TOC} is the available concentration
53 of a specific substrate as total organic carbon (mg L^{-1}), T_{TOC} is the total available organic carbon
54 concentration (mg L^{-1}), r_i is the degradation rate of compound i when present in a mixture, and r_0
55 is its degradation rate when present alone. Thus, $r_i = f \times r_0$ (Gomez et al., 2008).

56 Principles and concepts regarding the use of multiple substrates are more easily
57 developed under simple laboratory conditions; however, they have to be validated in real, natural
58 environments. Conditions leading to sequential substrate degradation have different time scales,
59 and therefore, might lead to different observations in the field. In addition, due to differences in
60 the dilution processes, rates of biodegradation and changes in redox conditions, it is very difficult
61 to design laboratory experiments to encompass the complex dynamics of biodegradation in the
62 subsurface. This suggests the need for long-term field studies to determine the effect of ethanol
63 preferential degradation on the attenuation of BTEX compounds.

64 This study evaluates at the field scale how substrate proportions influence biodegradation
65 of ethanol and BTEX in groundwater, in two controlled release experiments under different
66 redox conditions. Field data are compared with computer simulations using the Modular Three-
67 Dimensional Finite Difference Groundwater Flow (MODFLOW; Harbaugh et al., 2000),
68 Reactive Transport in 3 Dimensions (RT3D; Clement, 1997), and the General Substrate
69 Interactions Module (GSIM; Gomez et al., 2008). These simulations of the dynamics of ethanol

70 and BTEX plumes were used to assess the validity of the metabolic flux dilution model, and to
71 gain fundamental insight to recommend practical solutions to accelerate BTEX biodegradation
72 (e.g., add nitrate to increase the electron acceptor pool and stimulate faster degradation of
73 ethanol and other easily degradable substrates that hinder BTEX biodegradation).

74

75 **MATERIALS AND METHODS**

76 Two controlled releases of Brazilian gasoline (ethanol content 24% v/v) were considered:
77 one under natural attenuation (MNA) and the other under nitrate biostimulation (NB) conditions
78 (Figure 1). A detailed description of the experiments is presented elsewhere (Corseuil et al.,
79 2011; Da Silva and Corseuil, 2012). Briefly, the experimental areas are located in the Ressacada
80 Farm, Florianópolis, SC, Brazil (Latitude: 27°30'S, Longitude: 48°30'W). Climate in the region
81 is mesothermic humid with an annual average precipitation of 1600 mm. Regional geology is
82 characterized by unconsolidated deposits of eolian, alluvial, lacustrine and marine sands with
83 less than 5% of silt and clay. Each release consisted of one pulse of 100 L at the groundwater
84 table level. Initial masses of benzene, toluene, ethylbenzene and total xylenes released were 355,
85 2,234, 680 and 3,756 g, respectively. The releases were 400 m apart to avoid co-mingling.
86 Groundwater seepage velocity was approximately 3.1 m year⁻¹ and 5.1 m year⁻¹, respectively, for
87 the MNA and NB experiments. For the NB experiment, 5 L of a solution containing sodium
88 nitrate and potassium dihydrogen phosphate (4 g L⁻¹) was injected into six injection wells
89 upstream of the source zone three times a week for approximately 9 months after the release.

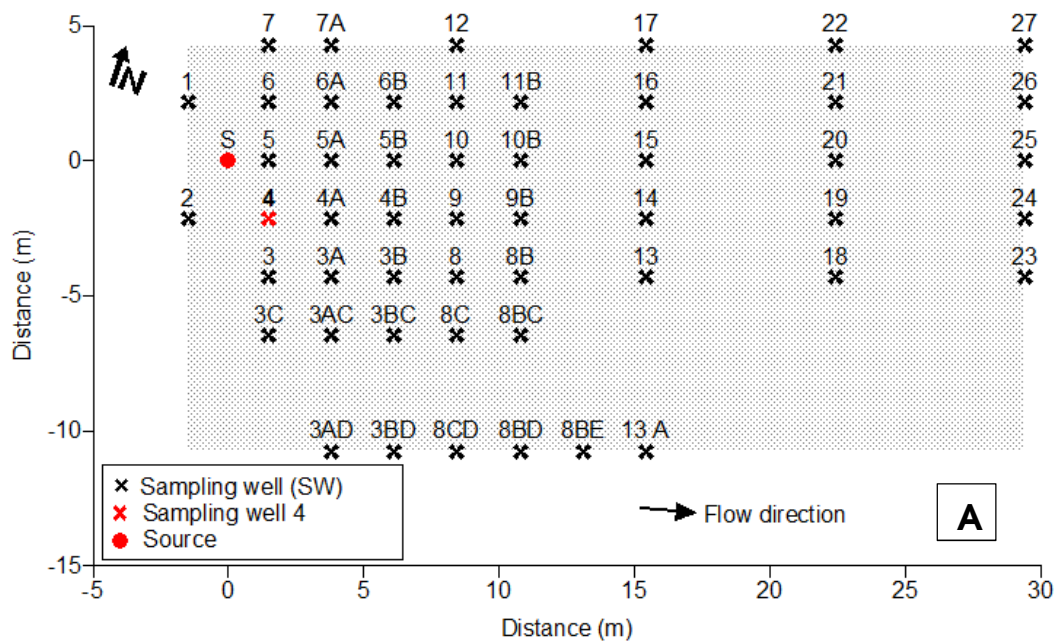
90 Groundwater monitoring was performed using multilevel sampling wells (SW) installed
91 perpendicular to groundwater flow direction. Data used to evaluate multiple substrate

92 interactions were located at SW4 approximately 2.0 m downgradient of the source at 2.0 m
 93 below ground surface (bgs) for the MNA experiment and 2.3 m bgs for the NB experiment.

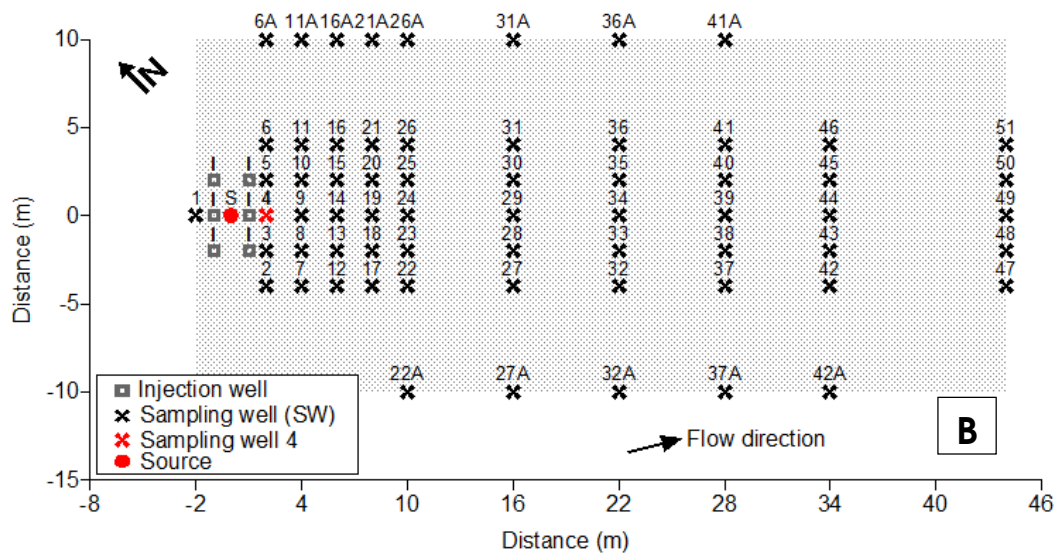
94 Dissolved total organic carbon (T_{TOC} , expressed as mg TOC L⁻¹) included ethanol, BTEX
 95 and acetate, which is a common byproduct of ethanol degradation. However, acetate represented
 96 less than 2% and 1% of T_{TOC} in the MNA and NB experiments, respectively, thus exerting minor
 97 contribution to metabolic flux dilution.

98 Pseudo-first-order decay coefficients were determined for BTEX after the lag period
 99 (about 1.7 years for MNA and 3 years for the NB release), by fitting the concentration versus
 100 time data from SW4 to an exponential decay model. Background groundwater concentrations of
 101 geochemical parameters are presented in Table 1.

102



103



104

105

106

Figure 1. Schematic view of MNA (A) and NB (B) experimental areas configuration.

107

Table 1 – Background groundwater characteristics.

108

Variable	Value
Temperature (°C)	17 – 25
Redox Potential (ORP) (mV)	32 - 524
pH	4.0 – 5.3
Dissolved oxygen (DO) (mg L ⁻¹)	2.3 – 7.0
Nitrate (mg L ⁻¹)	0.05 – 1.6
Sulfate (mg L ⁻¹)	0.3 – 4.4
Iron (II) (mg L ⁻¹)	0.0 – 1.6
Phosphate (mg L ⁻¹)	0.1 – 0.5
Methane (mg L ⁻¹)	< 0.01

109

110

111

112

113

A General Substrate Interaction Model (GSIM), using Monod multiplicative kinetics, was used to evaluate 3-dimensional interactions between substrates (ethanol and BTEX) and microbial populations present in the soil. The GSIM model (Gomez et al., 2008) works as a module for RT3D (Clement, 1997), and requires groundwater flow conditions from MODFLOW

114 (Harbaugh et al., 2000). Together, these models incorporate common fate and transport processes
115 such as: advection, dispersion, adsorption, biodegradation and depletion of available electron
116 acceptors. The GSIM model further incorporates important, and often ignored, substrate
117 interaction processes between ethanol and BTEX compounds, which can cause slower
118 degradation rates of BTEX at sites with high ethanol concentrations (Lovanh and Alvarez, 2004).
119 These interactions include: (a) metabolic flux dilution (MFD; Lovanh and Alvarez, 2004), (b)
120 catabolite repression (CR; Madigan et al., 2000), and (c) changes in specific microbial
121 populations of ethanol/BTEX degraders. Metabolic flux dilution refers to a lower specific BTEX
122 utilization rate by microorganisms due to non-competitive inhibition by ethanol or other
123 preferentially degraded substrate (Lovanh and Alvarez, 2004). The model is capable of
124 simulating contaminant plume elongation and degradation over time, with the associated changes
125 in microbial populations following the traditional sequential development of different electron
126 accepting conditions (aerobic, nitrate reducers, iron reducers, sulfate reducers and methanogenic
127 microbes), associated with the depletion of corresponding electron acceptors. The model requires
128 as input contaminant concentrations over time at the source zone, and does not consider LNAPL
129 dissolution dynamics (Gomez et al., 2008).

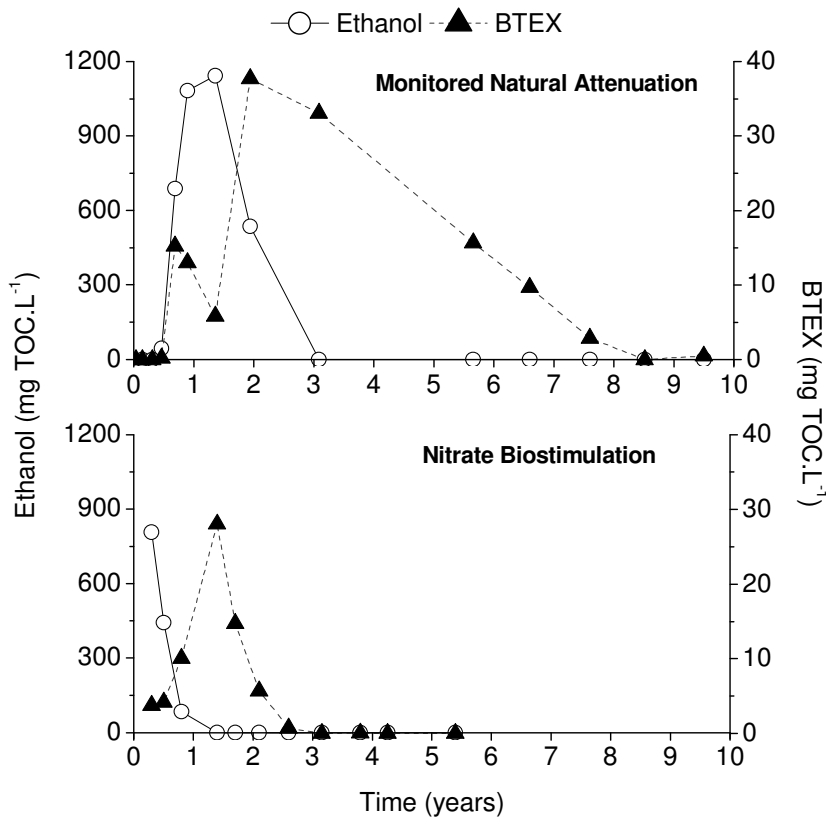
130 The Ressacada field site conditions were simulated in the RT3D/GSIM domain
131 considering a hydraulic conductivity of $1.1 \times 10^{-4} \text{ cm s}^{-1}$, effective aquifer porosity of 0.2, average
132 groundwater velocity of 3.1 m year^{-1} and average hydraulic gradient of 0.018 m/m (Corseuil et
133 al., 2011; Da Silva and Corseuil, 2012). Hydraulic flow conditions in the simulated domain, as
134 generated by MODFLOW, were corroborated by simulations with the MODPATH software
135 (Pollock, 1994). Particles generated by MODPATH similarly travelled 3.1 m over the course of
136 1 year of simulation time. Due to the complex source zone physical conditions, including a

137 variable height water table, source zone dissolution rates for ethanol and BTEX were estimated
138 using initial total mass (355 g for benzene and 18,900 g for ethanol). Biokinetic parameters for
139 ethanol and benzene degradation were based on those described by Gomez & Alvarez (2010),
140 modified for calibration of specific Ressacada site conditions (Table 3). The aquifer material has
141 an organic content (f_{oc}) of 0.06% (Corseuil et al., 2011), suggesting linear partitioning
142 coefficients (K_d) of $3.55 \times 10^{-13} \text{ mg m}^{-3}$ for ethanol and $4.24 \times 10^{-11} \text{ mg m}^{-3}$ for benzene.
143 Partitioning coefficients were calculated using the relationship $K_d = 0.63 \times f_{oc} \times K_{ow}$ (Karickhoff
144 et al., 1979) with water-octanol partition values obtained from the literature (Hilal et al., 2004).

145

146 **RESULTS AND DISCUSSION**

147 Converging lines of evidence indicate that biodegradation was largely responsible for the
148 significant decreases in ethanol and BTEX concentrations in both releases, after initial increases
149 associated with the dissolution and migration of the released fuel (Figure 2).



150

151 Figure 2. Dissolved TOC concentrations for ethanol and BTEX for the MNA (SW4, 2.0 m bgs)
 152 and NB (SW4, 2.3 m bgs) experiments.

153

154

155

156

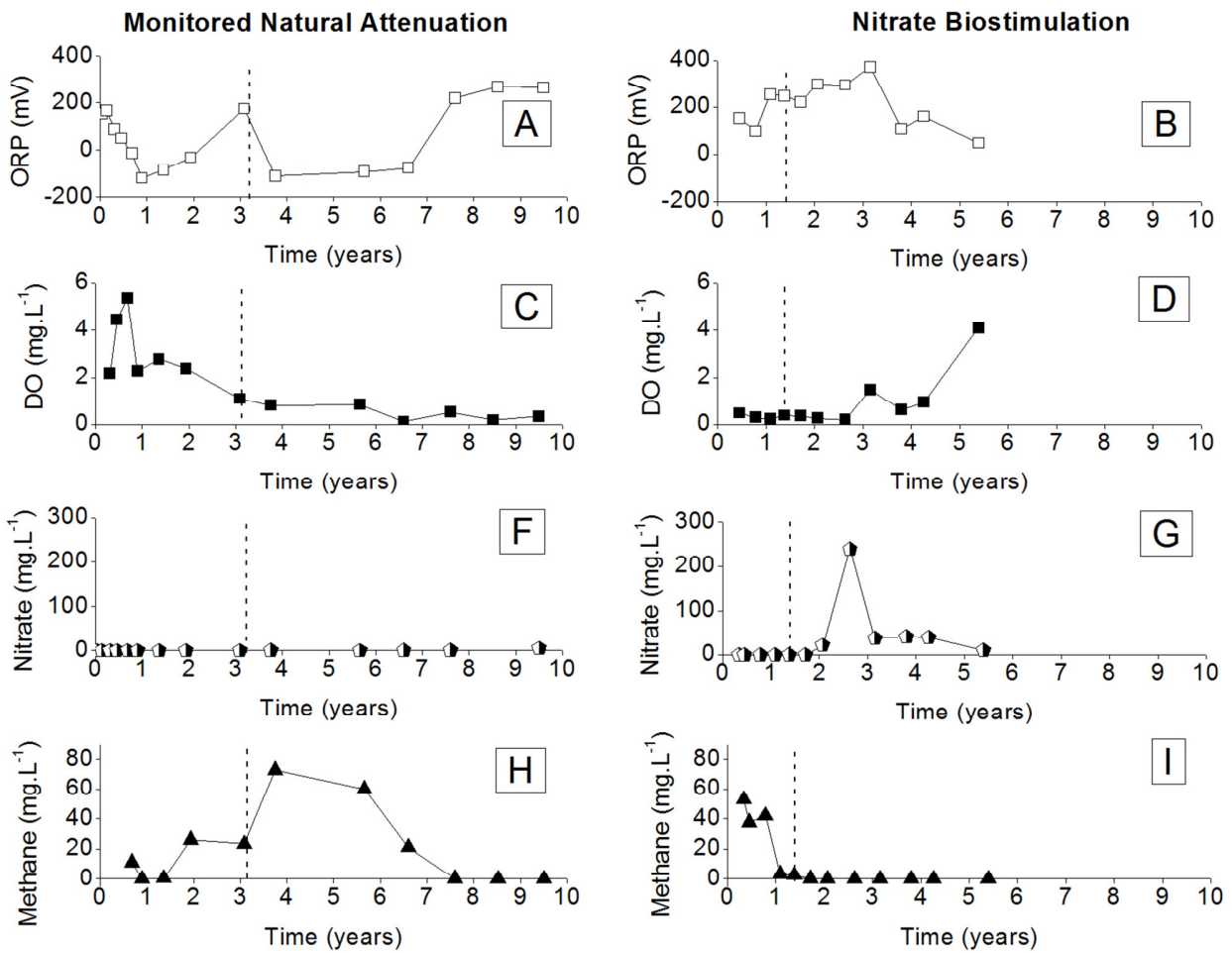
157

158

159

160

This evidence includes (1) the geochemical footprint; i.e., simultaneous consumption of released substrates (Figures 2) and electron acceptors with accompanying decrease in ORP and methane generation (for the MNA experiment) before rebounding to initial conditions after the release was attenuated (Figure 3); (2) an adequate fit of the data by model simulations (Figures 5 and 6) using typical biokinetic coefficients (Table 2); and (3) past studies demonstrating the corresponding indigenous biodegradation capabilities at this site (Corseuil et al., 2011; Da Silva et al., 2012).



161

162 Figure 3 – Redox potential (ORP) (A and B), dissolved oxygen (DO) (C and D), nitrate (E and F)

163 and methane (G and H) for the monitored natural attenuation experiment (SW4 2.0 m bgs) and

164 nitrate biostimulation experiment (SW4 2.3 m bgs). Dashed lines indicate onset of BTEX decay.

165

166

167

168

169

170

171
172

Table 2 - Biokinetic Parameters of Modeled Compounds.

	First-order degradation rate coefficient, λ (1/d)	Source	Maximum specific growth rate, μ_m (1/d)	Source	Half saturation constant, K_s (mg/l) ³	Source	Microbial cell yield, Y (g/g)	Source
Ethanol								
Aerobic	0.35	<i>Powers et al., 2001b</i>	11.04	<i>Lovanh et al., 2002</i>	63.09	Calculated ³	0.50	<i>Heulekian and Manganelli, 1951</i>
Nitrate Reducing	0.53	<i>Corseuil et al., 1998</i>	0.35	Calculated ²	0.25	Calculated ³	0.26	Calculated ²
Sulfate Reducing	0.10	<i>Corseuil et al., 1998</i>	0.21	Calculated ²	1.17	Calculated ³	0.18	Calculated ²
Iron Reducing	0.17	<i>Corseuil et al., 1998</i>	0.21	Calculated ²	0.67	Calculated ³	0.18	Calculated ²
Methanogenic	0.2	<i>Powers et al., 2001b</i>	0.16	Calculated ²	0.12	Calculated ³	0.07	<i>Lawrence and McCarty, 1969</i>
Benzene								
Aerobic	0.68	<i>Alvarez et al., 1991</i>	3.24	<i>Alvarez et al., 1991</i>	1.22	Calculated ³	0.39	<i>Grady et al. 1989</i>
Sulfate Reducing	0.02	<i>Kazumi et al., 1997; Wiedemeier et al., 1996; Rifai et al., 1995</i>	1.25	<i>Godeke et al, 2008</i>	3.25	Calculated ³	0.24	Calculated ²
Iron Reducing	0.00	<i>Wilson et al, 1990; Kazumi et al, 1997</i>	0.15	<i>Lovley and Lonergan, 1990</i>	3.05	Calculated ³	0.14	Calculated ²
Methanogenic	0.003	<i>Wilson et al, 1990; Kazumi et al, 1997</i>	0.30	<i>Ulrich and Edwards, 2003</i>	2.00	<i>O'Rourke, 1968</i>	0.05	<i>O'Rourke, 1968</i>
			Value				Source	
Other Parameters								
Aerobic Microbial Decay Rate (b_{Aer})			0.2 1/d	Based on mix culture aerobic systems [McCarty and Brodersen, 1962]				
Anaerobic Microbial Decay Rate (b_{An})			0.03 1/d	Based on methane fermentation [Lawrence and McCarty, 1969]				
Alcohol aerobic degraders initial population			10^6 cells/g-soil	<i>Chen et al., 1992</i>				
Alcohol anaerobic degraders initial population			10^5 cells/g-soil	10% of alcohol degrading aerobic populations				
Benzene aerobic degraders initial population			10^5 cells/g-soil	10% of total populations				
Benzene anaerobic degraders initial population			10^3 cells/g-soil	1% of Benzene degrading aerobic populations				

¹ First order degradation rates estimated on water half-lives of the compounds. [Howard et al., 1991]

² Values estimated using the Thermodynamic Electron Equivalents Model for Bacterial Yield Prediction [McCarty, 2007].

³ Values estimated on the basis of the relationship $\lambda = (\mu X/Y K_s)$ [Alvarez and Illman, 2006].

173
174

175 When an ethanol-blended fuel is released to the environment, the preferential degradation
176 of ethanol (which has a relatively simple molecular structure) can hinder BTEX degradation.
177 Potential inhibitory mechanisms include the depletion of favorable terminal electron acceptors

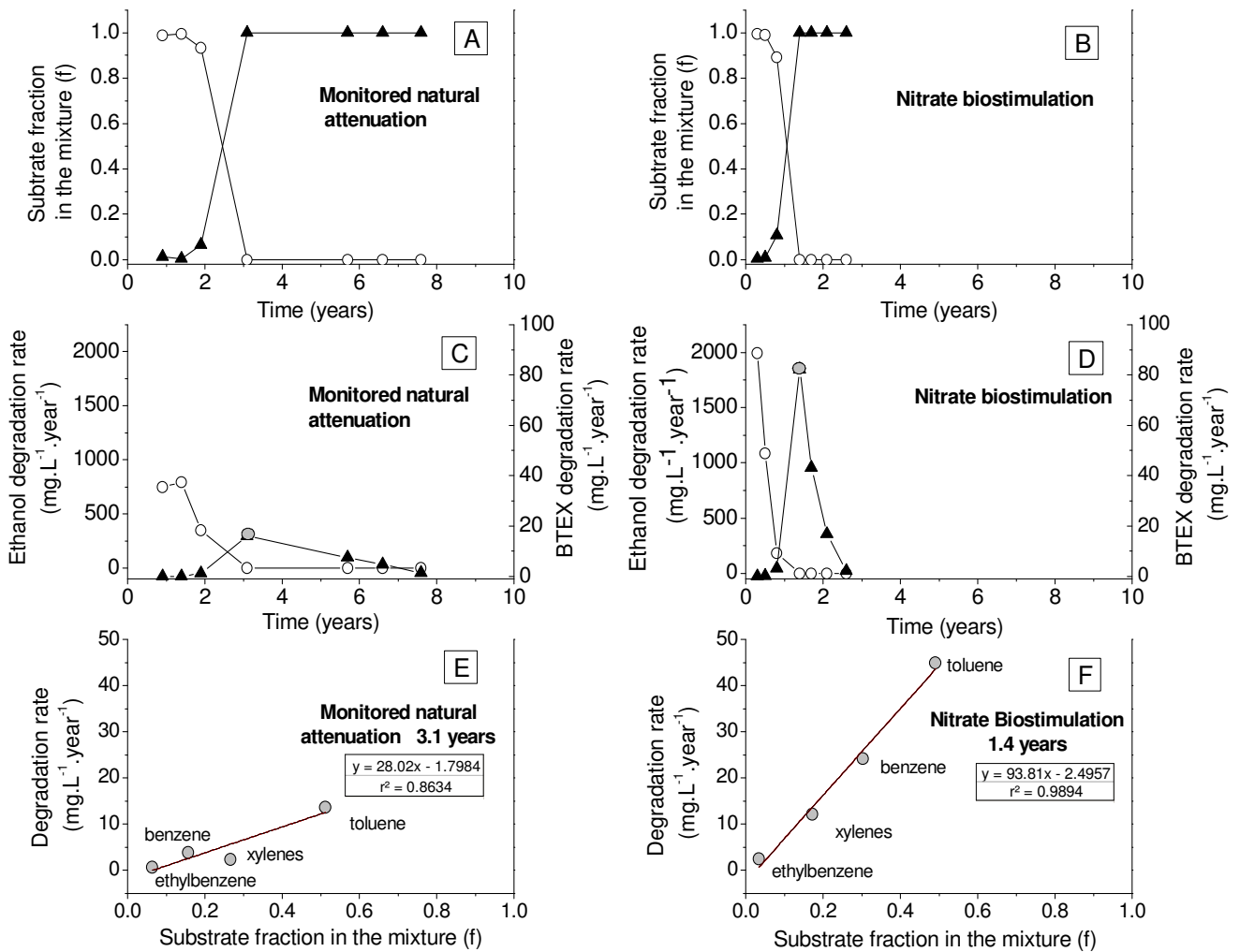
178 (e.g., dissolved oxygen) and nutrients during ethanol consumption, proliferation of microbial
179 populations that grow on ethanol but cannot degrade BTEX, thermodynamic constraints posed
180 by accumulation of fermentation products that are common to ethanol and BTEX degradation
181 pathways (e.g., acetate and H₂), catabolite repression and metabolic flux dilution (Gomez et al.,
182 2008; Cápiro et al., 2007; Lovanh & Alvarez, 2004; Da Silva & Alvarez, 2002). Previous
183 modeling studies showed that metabolic flux dilution can be the most influential inhibitory
184 mechanism for BTEX biodegradation in ethanol-blended fuel spills scenarios (Lovanh &
185 Alvarez, 2004; Gomez et al., 2008). Furthermore, the concept of metabolic flux dilution is
186 relatively simple to model at the reactor and field scales (Equation 1). Therefore, the metabolic
187 flux dilution model was used to analyze the release data.

188 For ethanol-blended fuel spills, initial aqueous concentrations of ethanol tend to be much
189 higher than BTEX concentrations. Ethanol concentrations near the source zones of the MNA and
190 NB releases reached about 2,000 mg L⁻¹ (1,100 mg-TOC L⁻¹), while maximum BTEX
191 concentrations were approximately 40 mg L⁻¹ (38 mg-TOC L⁻¹) (Figure 2), representing only 3%
192 of the total available substrate as dissolved TOC. Consequently, significant BTEX metabolic flux
193 by the more abundant ethanol would be expected, which would result in the apparent preferential
194 biodegradation of ethanol. Accordingly, BTEX concentrations started to decrease only after the
195 onset of ethanol removal, which occurred earlier in the NB experiment (after 1.4 years) than the
196 MNA experiment (after 3.0 years). The onset of BTEX degradation in both experiments occurred
197 when the metabolic dilution factor (*f*) approached 1 (Figure 4A and Figure 4B).

198 First-order decay constants (determined after the compound-specific onset of
199 biodegradation) are summarized in Table 3. These rate constants were significantly lower for the
200 MNA experiment (*k*= 0.76 ± 0.60 for benzene; 0.81 ± 0.97 for toluene; 0.33 ± 0.13 for

201 ethylbenzene, $0.28 \pm 0.14 \text{ year}^{-1}$ for xylenes and $0.71 \pm 0.43 \text{ year}^{-1}$ for ethanol) than for the NB
202 experiment ($k= 2.84 \pm 2.01$ for benzene; 3.27 ± 1.10 for toluene; 2.58 ± 0.52 for ethylbenzene,
203 $2.52 \pm 0.48 \text{ years}^{-1}$ for xylenes, and $2.48 \pm 1.96 \text{ years}^{-1}$ for ethanol). Nitrate addition to increase
204 the electron acceptor pool accelerated the biodegradation of ethanol, which resulted in earlier
205 onset of BTEX biodegradation (Figure 2). Nitrate amendment also resulted in a higher redox
206 potential and no methane was detected in the NB release (Figure 3). Moreover, nitrate
207 consumption was consistent with the onset of ethanol and BTEX biodegradation (Figure 3),
208 providing evidence that nitrate reduction was the main biodegradation pathway in NB
209 experiment.

210



211
 212 Figure 4. Ethanol (○) and BTEX (▲) as TOC fractions in the mixture (calculated according to
 213 equation 1) for the MNA (SW4 2.0 m bgs) (A) and NB (SW4 2.3 m bgs) (B) experiments.
 214 Ethanol (○) and BTEX (▲) degradation rates ($r_i = f \times r_0$) as a function of time after the release in
 215 MNA (C) and NB (D) experiments. BTEX compounds degradation rate ($r_0 = k C$) after ethanol
 216 depletion (●) and their relative fraction in the mixture for the MNA (E) and NB (F) experiments.

217
 218 The metabolic flux dilution model predicts that specific removal rates should be
 219 proportional to the fraction of the available substrates in the mixture (equation 1). BTEX

220 degradation follows this trend (Figure 4, panels E and F; $r^2 \geq 0.9$). More favorable
 221 thermodynamic conditions for biodegradation under NB conditions resulted in higher
 222 degradation rates (maximum of 2,000 and 82 mg L⁻¹.year⁻¹ for ethanol and BTEX, respectively)
 223 relative to MNA (maximum of 800 and 16 mg L⁻¹.year⁻¹ for ethanol and total BTEX,
 224 respectively). Furthermore, the faster removal of ethanol in the NB experiment (at 1.4 years
 225 compared to 3.1 years for MNA) resulted in a faster disappearance of its inhibitory effect (i.e.,
 226 metabolic flux dilution) and an earlier onset of BTEX biodegradation. These observations are in
 227 accordance with previous laboratory studies (Dou et al., 2008; Lendemann et al. 1996; Lovanh et
 228 al. 2002; Lovanh & Alvarez, 2004).

229

230 Table 3 – BTEX Pseudo-first-order attenuation constants (k) near the source zones (SW4) for the
 231 natural attenuation and nitrate biostimulation experiments

Experiment	Substrate	Timeframe^a (years)	k (year⁻¹)	R²	n	p-value
Monitored Natural Attenuation	Benzene	3.1 to 7.6	0.76 ± 0.60	0.84	5	< 0.05
	Toluene	3.1 to 7.6	0.81 ± 0.97	0.94	5	< 0.05
	Ethylbenzene	3.1 to 7.6	0.33 ± 0.13	0.95	5	< 0.05
	Xylenes	3.1 to 7.6	0.28 ± 0.14	0.93	5	< 0.05
	Ethanol	1.0 to 3.7	0.71 ± 0.43	0.96	4	< 0.05
Nitrate Biostimulation	Benzene	1.4 to 2.6	2.84 ± 2.01	0.95	4	< 0.05
	Toluene	1.4 to 2.6	3.27 ± 1.10	0.99	4	< 0.05
	Ethylbenzene	1.4 to 2.6	2.58 ± 0.52	1.00	4	< 0.05
	Xylenes	1.4 to 2.6	2.52 ± 0.48	1.00	4	< 0.05
	Ethanol	0.3 to 2.1	2.48 ± 1.96	0.94	4	< 0.05

232 ^a Period after gasohol release. The timeframes correspond to the highest compound
 233 concentration until its depletion.

234

235 Field data from both experiments were simulated using GSIM model. Using data from the
236 MNA experiment to calibrate the source zone LNAPL dissolution rates and the GSIM model half
237 saturation coefficients for Ethanol and Benzene (K_S , Table 2), the calculated total plume mass
238 over time was accurately simulated for both ethanol and benzene (Figure 5). Calculated R^2
239 values are 0.87 and 0.80 for ethanol and benzene respectively. Simulated contaminant
240 concentrations at SW4 (Figures 5c and 5d) fit the observed patterns with R^2 of 0.69 and 0.51 for
241 ethanol and benzene respectively. Modeled accuracy was hindered by coarse model domain cell
242 resolution (1 m \times 1 m in XY plane), which are required for feasible execution times, and to
243 significant spread of the field data, particularly for benzene measurements. Nevertheless, the
244 model adequately simulated peak concentration values at point SW4 and concentration evolution
245 over time (Figure 5).

246

247

248

249

250

251

252

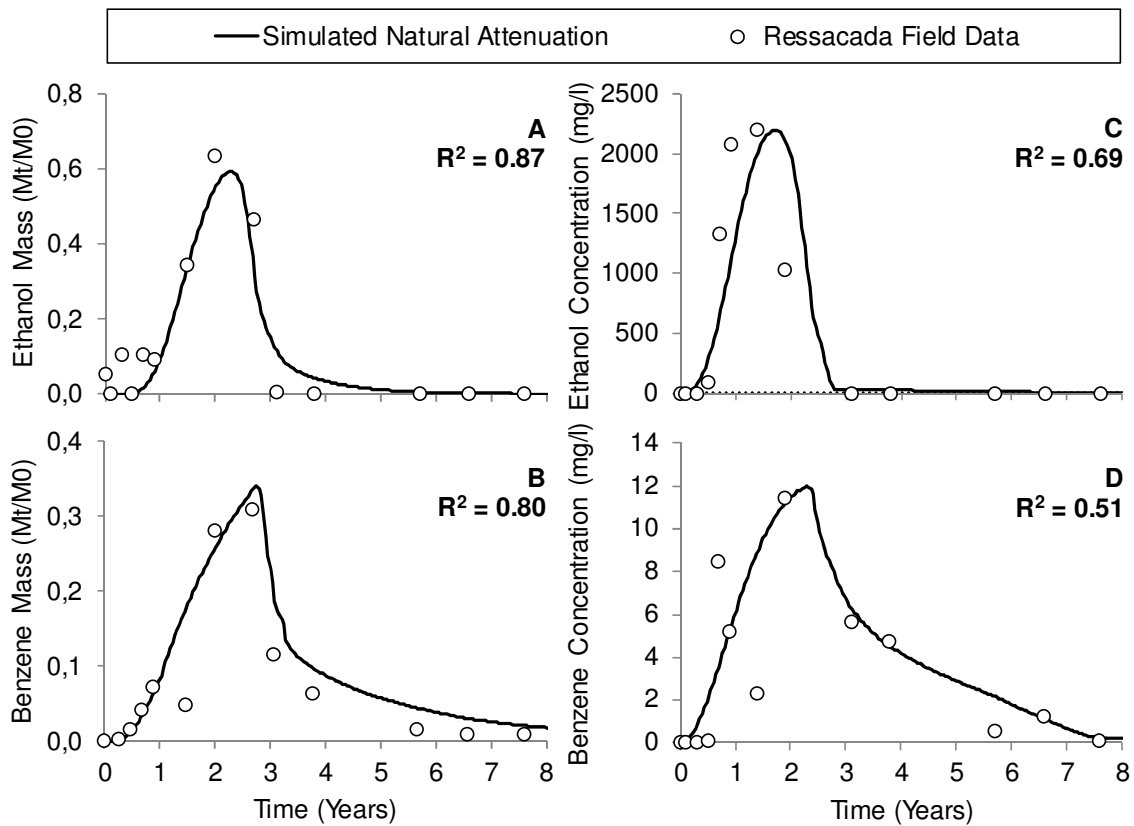
253

254

255

256

257



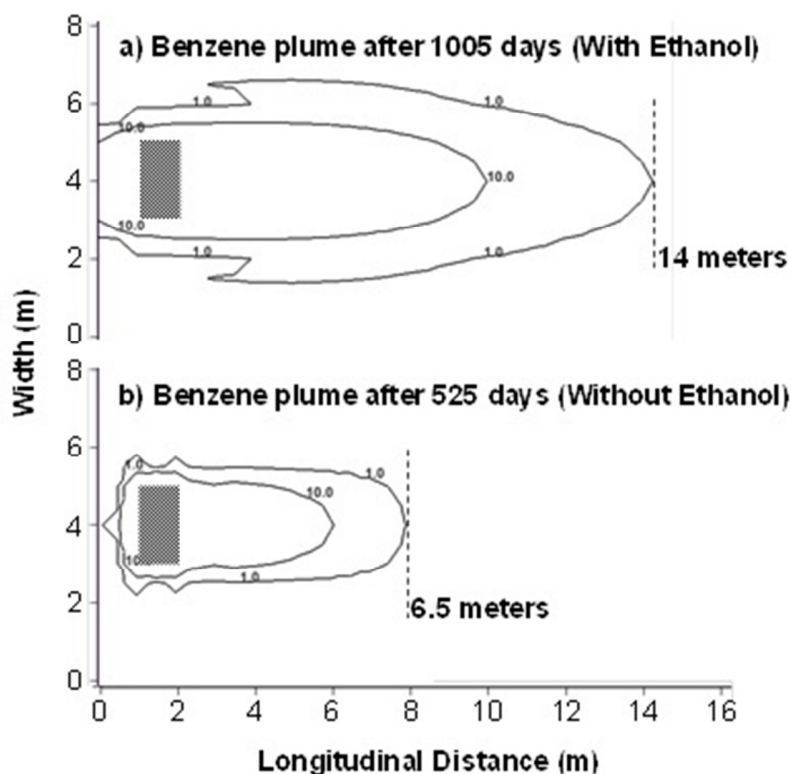
258

259 Figure 5 – Comparison of natural attenuation simulation using GSIM (solid line) with Ressacada
 260 field data (dots), considering: (A) Ethanol plume total mass ($R^2 = 0.87$); (B) Benzene plume total
 261 mass ($R^2 = 0.80$); (C) Ethanol concentration over time at point SW4 ($R^2 = 0.69$); and (D)
 262 Benzene concentration over time at Point SW4 ($R^2 = 0.51$).

263

264 The total contaminant plume mass in the system (Figures 5a and 5b) was correctly
 265 simulated to increase initially due to ethanol and benzene source zone dissolution, reaching a
 266 peak after about 2 years of simulation time, at which point degradation and diffusion processes
 267 dominate and the total dissolved mass begins to decrease. The total dissolved ethanol mass is
 268 significantly reduced by year 3, and ethanol disappears from the system by year 5. Benzene mass

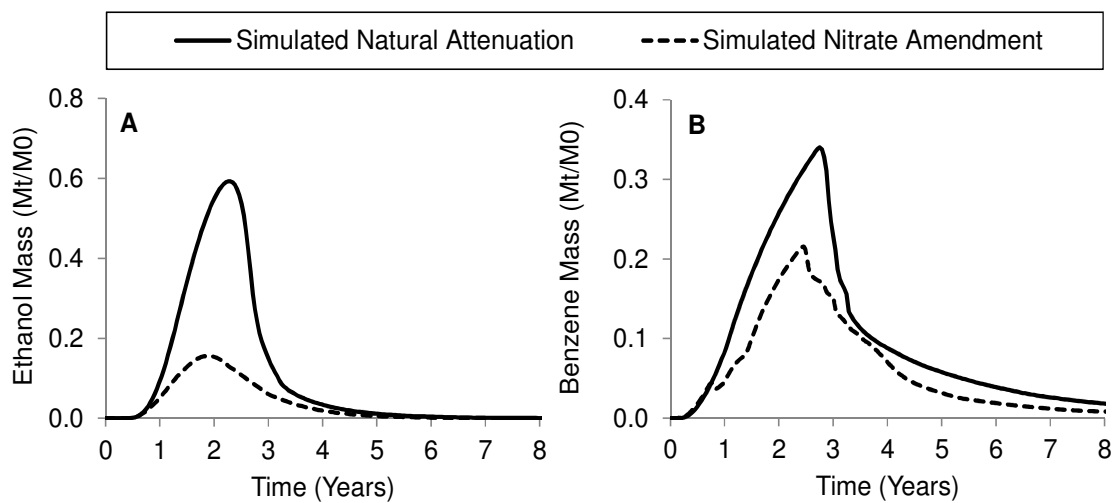
269 removal increases markedly once ethanol disappears from the system. The simulated maximum
270 plume lengths (1 mg L^{-1} contours) reach 19 m for ethanol and 14.5 m for benzene. This is
271 significantly longer (8 m increase) than the simulated plume length for benzene alone at these
272 concentrations (Figure 6).



273
274 Figure 6. Maximum benzene plume length reached using the GSIM model, with and without
275 ethanol in the system: (a) 14 meters for the 1 mg L^{-1} contour with ethanol present after 1005
276 days; (b) 6.5 meters for the 1 mg L^{-1} contour without ethanol present after 525 days. Source zone
277 is shown as grey area.

278
279 The benefits of nitrate addition to enhance ethanol biodegradation and mitigate its
280 inhibitory effect on BTEX degradation are evident by comparing GSIM simulations of MNA
281 versus NB conditions (Figure 7). Using a constant near-source zone concentration of 80 mg L^{-1}

282 of nitrate results in a reduction of 74% for ethanol total plume mass (Figure 7a). A 53%
 283 reduction of the benzene total plume mass present in the system over time was also observed
 284 (Figure 7b). Benzene mass reduction corroborates that the presence of ethanol in the system
 285 hinders benzene natural attenuation. These results are in agreement with the metabolic flux
 286 dilution model (Lovanh and Alvarez, 2004; Madigan et al., 2000; Gomez et al., 2008), which
 287 adequately simulated ethanol and benzene plume dynamics for these two releases under different
 288 redox conditions. Since metabolic flux dilution proved to be suitable to model MNA and NB
 289 field data and that proportionality among substrates fraction in the mixture and degradation rates
 290 was demonstrated, it is plausible to infer that the late BTEX biodegradation relative to ethanol
 291 was influenced by its relative contribution to the mixture.



292
 293 Figure 7. Comparison of total plume mass (M_t) present in the simulation domain over time,
 294 shown as a ratio of the total contaminant mass injected in the system (M_0), for simulated natural
 295 attenuation versus nitrate biostimulation. (A) Nitrate amendment results in a 74% increase in
 296 ethanol degradation; (B) Nitrate amendment results in a 53% increase in benzene degradation.

297

298 **CONCLUSIONS**

299 Previous studies of ethanol-blended fuel releases indicated that ethanol can delay BTEX
300 degradation independently of redox conditions. This study shows that the apparent preferential
301 degradation of ethanol may be largely explained by the metabolic flux dilution model, which
302 considers the simultaneous degradation of multiple substrates with compound-specific
303 degradation rates being proportional their relative abundance in the mixture. Accordingly, the
304 metabolic flux dilution factor used to simulate non-competitive inhibition in the presence of
305 alternative substrates (previously presented for lab-scale batch and continuous flow experiments)
306 was shown to be applicable to complex, field-scale systems involving subsurface spills of
307 ethanol-blended fuel. However, caution should be exercised in recognizing the limitations of
308 this model (Gomez et al., 2008): microbial growth is assumed to as fully penetrated biofilms in
309 the aquifer matrix with no attachment/detachment kinetics (Chen et al., 1992, Harvey et al.,
310 1984; Lehman et al., 2001); biological degradation activity occurs in the liquid phase, and decay
311 of sorbed constituents is ignored; dissolved total organic carbon is assumed to be fully available
312 to microorganisms; the model does not consider degradation byproducts such as acetate or
313 propionate; the model does not consider complex capillary zone transport behavior of high
314 alcohol content mixtures.

315 One important practical implication of this work is that the initial focus of effort to
316 remediate releases of ethanol-blended fuel (after free-product recovery) should be to accelerate
317 the degradation of ethanol (e.g., by augmenting the electron acceptor pool through stoichiometric
318 nitrate addition). This would more rapidly decrease the fraction of ethanol in the mixture and
319 speed up the biodegradation of BTEX that are the main regulatory drivers.

320

321 **ACKNOWLEDGMENTS**

322 This research was funded primarily by Petróleo Brasileiro S/A – PETROBRAS.
323 Additional funds (scholarships) were provided by Coordination of Improvement of Higher
324 Education Personnel (CAPES) and the National Council for Scientific and Technological
325 Development (CNPq). The authors also thank students, technicians and researchers that directly
326 or indirectly helped for the development and monitoring of the experiments.

REFERENCES

- Alvarez, P.J.J. & Illman, W.A. (2006). *Bioremediation and Natural Attenuation of Groundwater Contaminants: Process Fundamentals and Mathematical Models*. John Wiley & Sons. ISBN No. 0-471-65043-9. 608 p.
- Bielefeldt, A.R.; Stensel, H.D. (1999) Modeling competitive inhibition effects during biodegradation of BTEX mixtures. *Water Research*, 33 (3): 707-714.
- Chen, Y., L. M. Abriola, P. J. J. Alvarez, P. J. Anid, and T. M. Vogel (1992), Modeling transport and biodegradation of benzene and toluene in sandy aquifer material: Comparisons with experimental measurements, *Water Resour. Res.*, 28(7), 1833– 1847
- Chen, Y. D., Barker, J.F., Gui, L., (2008). A strategy for aromatic hydrocarbon bioremediation under anaerobic conditions and the impacts of ethanol: A microcosm study. *J. Contam. Hydrol.* 96, 17-31.
- Clement, T. P., (1997). RT3D - A Modular Computer Code for Simulating Reactive Multi-species Transport in 3-Dimensional Groundwater Systems - Publication PNNL-11720 (pp. 1– 59). Pacific Northwest National Laboratory, Richland, Washington 99352.
- Corseuil, H.X., Hunt, C.S., Dos Santos, R.C.F., Alvarez, P.J.J., (1998). The influence of the gasoline oxygenate ethanol on aerobic and anaerobic BTX biodegradation. *Water Res.* 32, 2065-2072.
- Corseuil, H.X., Monier, A.,L., Fernandes, M., Schneider, M.R., Nunes, C., Do Rosário, M., Alvarez, P.J.J., (2011). BTEX Plume Dynamics Following an Ethanol Blend Release: Geochemical Footprint and Thermodynamic Constraints on Natural Attenuation. *Environ. Sci. & Technol.* 45, 3422-3429.
- Da Silva, M.L.B. & Alvarez, P.J.J. (2002) Effects of Ethanol versus MTBE on Benzene, Toluene, Ethylbenzene, and Xylene Natural Attenuation in Aquifer Columns. *Journal of Environmental Engineering*. 128 (9): 862–867.
- Da Silva, M.L.B., Alvarez, P.J.J., (2004). Enhanced Anaerobic Biodegradation of Benzene-Toluene-Ethylbenzene-Xylene–Ethanol Mixtures in Bioaugmented Aquifer Columns. *Appl. Environ. Microbiol.* 70, 4720–4726.
- Da Silva, M.L.B., Corseuil, H.X., (2012). Groundwater microbial analysis to assess enhanced BTEX biodegradation by nitrate injection at a gasohol-contaminated site. *Int. Biodeter. Biodegr.* 67, 21-27.
- Dou, J., Liu, X., Hu, Z., (2008). Anaerobic BTEX degradation in soil bioaugmented with mixed consortia under nitrate reducing conditions. *J. Environ. Sci.* 20, 585-592.

- Egli, T. (1995). The ecological and physiological significance of the growth of heterotrophic microorganisms with mixtures of substrates. *Adv. Microbiol. Ecol.* 14, 797-806.
- Freitas, J.G.; Mocanu, M.T.; Zoby, J.L.G.; Molson, J.W.; Barker, J.F. (2011) Migration and fate of ethanol-enhanced gasoline in groundwater: A modelling analysis of a field experiment. *Journal of Contaminant Hydrology*, 199 (1-4): 25-43.
- Goldemberg, J. (2007). Ethanol for a sustainable energy future. *Science*, 315(5813), 808–810.
- Gomez, D. E., De Blanc, P. C., Rixey, W. G., Bedient, P. B., & Alvarez, P. J. J. (2008). Modeling benzene plume elongation mechanisms exerted by ethanol using RT3D with a general substrate interaction module. *Water Resour. Res.*, 44(5), 1–12.
- Gomez, D. E., & Alvarez, P. J. J. (2010). Comparing the effects of various fuel alcohols on the natural attenuation of benzene plumes using a general substrate interaction model. *Journal of contaminant hydrology*, 113(1-4), 66–76.
- Harbaugh, B. A. W., Banta, E. R., Hill, M. C., & McDonald, M. G. (2000). MODFLOW-2000 , THE U . S. Geological Survey Modular Ground-Water Model — User Guide To Modularization Concepts And The Ground-Water Flow Process.
- Harvey, R. W., R. L. Smith, and L. George (1984). Effect of organic contamination upon microbial distributions and heterotrophic uptake in a Cape Cod, Mass. aquifer, *Appl. Environ. Microbiol.*, 48(6), 1197– 1202.
- Hilal, S.H.; Carreira, L.A. & Karickhoff, S.W. (2004) Prediction of the Solubility, Activity Coefficient, Gas/Liquid and Liquid/Liquid Distribution Coefficients of Organic Compounds. *QSAR & Combinatorial Science*, 23 (9): 709-720.
- Karickhoff, S.W., Brown, D.S., Scott T.A. (1979). Sorption of hydrophobic pollutants on natural sediments. *Water. Res.* 13, 241-248.
- Lehman, R. M., F. S. Colwell, and G. A. Bala (2001), Attached and unattached microbial communities in a simulated basalt aquifer under fracture- and porous-flow conditions, *Appl. Environ. Microbiol.* 67(6), 2799 – 2809.
- Lendenmann, U., Snozzi, M., Egli, T., (1996). Kinetics of the Simultaneous Utilization of Sugar Mixtures by *Escherichia coli* in Continuous Culture. *Appl. Environ. Microbiol.* 62, 1493-1499.
- Lovanh, N., Alvarez, P.J.J. (2004). Effect of Ethanol, Acetate, and Phenol on Toluene Degradation Activity and *tod-lux* Expression in *Pseudomonas putida* TOD102: Evaluation of the Metabolic Flux Dilution Model. *Biotechnol. and Bioeng.* 86, 801-808.

Lovanh, N., Hunt, C.S., Alvarez, P.J.J., (2002). Effect of ethanol on BTEX biodegradation kinetics: aerobic continuous culture experiments. *Water Res.* 36, 3739-3746.

Mackay, D.M., De Sieyes, N.R., Einarson, M.D., Feris, K.P., Pappas, A.A., Wood, I.A., Jacobson, L., Justice, L.G., Noske, M.N., Scow, K.M., Wilson, J.T., (2006). Impact of Ethanol on the Natural Attenuation of Benzene, Toluene, and *o*-Xylene in a Normally Sulfate-Reducing Aquifer. *Environ. Sci. & Technol.* 40, 6123-6130.

Madigan, J. T., J. M. Martinko, and J. Parker (2000), *Brock Biology of Microorganisms*, 9th ed., Prentice-Hall, Upper Saddle River, N. J.

Pollock, D.W., (1994) *User's Guide for MODPATH/MODPATH-PLOT, Version 3: A particle tracking post-processing package for MODFLOW, the U.S. Geological Survey finite-difference ground-water flow model: U.S. Geological Survey Open-File Report 94-464*, 6 ch.

Ruiz-Aguilar, G.M., Fernandez-Sanchez, J.M., Kane, S.R., Kim, D., Alvarez, P.J.J., (2002). Effect of ethanol and methyl-tert-butyl ether on monoaromatic hydrocarbon biodegradation: response variability for different aquifer materials under various electron-accepting conditions. *Environ. Toxicol. Chem.* 21, 2631-2639.

Schaefer, C.E., Yang, X., Pelz, O., Tsao, D.T., Streger, S.H., Stefan, R.J., (2010). Anaerobic biodegradation of iso-butanol and ethanol and their relative effects on BTEX biodegradation in aquifer materials. *Chemosphere.* 81, 1111-1117.